Crystals of Bound States in the Magnetization Plateaus of the Shastry-Sutherland Model

Philippe Corboz[1] and Frédéric Mila[2]
[1]Theoretische Physik, ETH Zürich, CH-8093 Zürich, Switzerland
[2]Institut de Théorie des Phénomènes Physiques, École Polytechnique Fédérale de Lausanne (EPFL), CH-1015 Lausanne, Switzerland
(Received 14 January 2014; revised manuscript received 5 March 2014; published 10 April 2014)

Using infinite projected entangled-pair states, we show that the Shastry-Sutherland model in an external magnetic field has low-magnetization plateaus which, in contrast to previous predictions, correspond to crystals of bound states of triplets, and not to crystals of triplets. The first sizable plateaus appear at magnetization $1/8$, $2/15$ and $1/6$, in agreement with experiments on the orthogonal-dimer antiferromagnet $SrCu_2(BO_3)_2$, and they can be naturally understood as regular patterns of bound states, including the intriguing $2/15$ one. We also show that, even in a confined geometry, two triplets bind into a localized bound state with $S_z = 2$. Finally, we discuss the role of competing domain-wall and supersolid phases, as well as that of additional anisotropic interactions.

DOI: 10.1103/PhysRevLett.112.147203 PACS numbers: 75.10.Jm, 02.70.-c, 75.10.Kt, 75.40.Mg

Predicting the phases of frustrated spin systems is one of the major challenges in theoretical condensed matter physics [1]. A famous example is the Shastry-Sutherland model (SSM)[2], which is believed to accurately capture the physics of the orthogonal-dimer antiferromagnet $SrCu_2(BO_3)_2$. A substantial effort has been invested in understanding the appearance of various magnetization plateaus observed in experiments [3–13]. Early on it was found that the SSM has almost localized triplet excitations [5,14], which suggests that each plateau corresponds to a particular crystal of localized triplets. This viewpoint has been supported by many analytical and (approximate) numerical studies over the last 15 years [14–25].

The SSM is given by the Hamiltonian

$$H = J\sum_{\langle i,j\rangle} \boldsymbol{S}_i \cdot \boldsymbol{S}_j + J'\sum_{\langle\langle i,j\rangle\rangle} \boldsymbol{S}_i \cdot \boldsymbol{S}_j - h\sum_i S_i^z, \qquad (1)$$

where the $\langle i, j\rangle$ bonds with coupling strength J build an array of orthogonal dimers, the bonds with coupling J' denote inter-dimer couplings, and h is the strength of the external magnetic field.

The main result of this Letter is that—in contrast to the standard belief—the plateaus are not crystals of $S_z = 1$ triplets [see Fig. 1(a)], but of $S_z = 2$ bound states of triplets, which form a pinwheel pattern as shown in Fig. 1(b), and which are shown to be stable even if they are localized. Bound states have previously been predicted to be relevant in the dilute limit of excitations [16,26–29], but not for the formation of crystals. The only hint so far that bound states can form crystals was found in a one-dimensional analog—a SSM spin tube [30]. It is also shown that the crystals formed by the bound states naturally explain the sequence of magnetization plateaus observed in $SrCu_2(BO_3)_2$. In particular, the 2/15 plateau is made of a simple and regular pattern of bound states, in contrast to the more complicated patterns of triplets which were previously suggested [12,21,24].

Method.—Our results have been obtained with infinite projected entangled-pair states (iPEPS), a variational tensor-network ansatz to represent a two-dimensional wave function in the thermodynamic limit [31–33]. It consists of a cell of tensors which is periodically repeated on the lattice; in the present work we use one tensor per dimer. Each tensor has five indices, a physical index for the local Hilbert space of a dimer, and four auxiliary indices which connect to the four nearest-neighboring tensors. Each tensor contains $4D^4$ variational parameters, where D is the dimension of an auxiliary index called the bond dimension which controls the accuracy of the ansatz. A $D = 1$ iPEPS simply corresponds to a site-factorized wave function (a product state), and by increasing D, quantum fluctuations can be systematically added to the state. A $D = 2$ iPEPS includes short-range quantum fluctuations and often qualitatively reproduces the results from linear

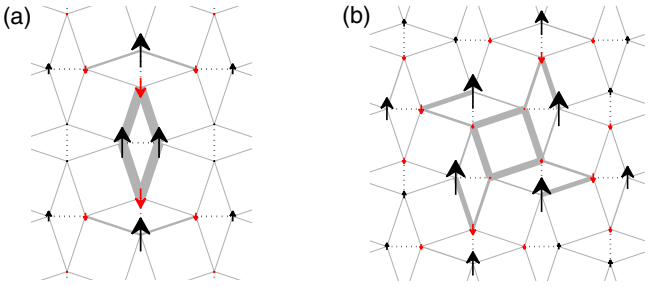

FIG. 1 (color online). Spin structures of two types of excitations in the SSM obtained with iPEPS: (a) elementary triplet ($S_z = 1$) excitation (obtained in a 6×6 unit cell), (b) bound state of triplets ($S_z = 2$) forming a pinwheel pattern (obtained in a 4×4 unit cell). The thickness of the next–nearest neighbor bonds is proportional to the square of the bond energy (all the thick bonds have a negative energy).

spin-wave (or flavor-wave) theory [34–36]. Here we consider iPEPS with D up to 12, which enables us to represent highly entangled states.

By using different cell sizes, iPEPS can represent different translational symmetry broken states (e.g., the different crystal structures). The tensors are either initialized randomly (this is how we found the bound states), or in a specific initial product state, e.g., corresponding to a particular triplet crystal. The latter states are typically metastable; i.e., we can increase D and the state remains in the particular initial state. In this way we can compare the variational energies of different candidate ground states.

For more details on the method we refer to Refs. [13,37] where we used the same approach for the SSM at zero and at high magnetic fields. For the experts we note that the optimization of the tensors (i.e., finding the best variational parameters) has been done via an imaginary time evolution. Most of the results have been obtained with the so-called simple update [38,39], which gives a reasonably good estimate of the energy, but we checked several simulations with the more accurate (and computationally more expensive) full update (see Ref. [33] for details). The contraction of the infinite tensor network is done with the corner-transfer matrix method [37,40,41]. For the plateau phases we used tensors with U(1) symmetry to increase the efficiency [42,43].

Ground state in the 1/8 plateau.—We focus on the 1/8 plateau in the physically relevant regime for $SrCu_2(BO_3)_2$, $J'/J = 0.63$, as a first example to show that crystals made of bound states have a lower variational energy than crystals made of triplets. Two triplet crystals have been proposed: the diamond pattern shown in Fig. 2(a) with basis vectors $v_1 = (2, -2)$ and $v_2 = (2, 2)$ [12,20,24], and a rhomboid pattern defined by $v_1 = (2, -2)$ and $v_2 = (3, 1)$ [6,7,10,20] (see also Supplemental Material [44]). In Fig. 2(c) we compare their variational energies with that of two different crystals of bound states: a square one with basis vectors $v_1 = (4, 0)$, $v_2 = (0, 4)$ [44] and a rhomboid one with basis vectors $v_1 = (4, 2)$, $v_2 = (0, 4)$ [Fig. 2(b)]. For $D = 2$ the diamond pattern of triplets has the lowest variational energy. This indicates that triplet crystals are favored if only low-order quantum fluctuations on top of a product state are taken into account. However, as soon as $D \geq 3$, the bound-state crystals are energetically lower than the triplet crystals. The two bound-state crystals are nearly degenerate, the rhomboid one being slightly below the square one. Bound-state crystals are also favored for other values of J'/J, as shown in the inset of Fig. 2(c).

Ground state in the 1/6 plateau.—We made a similar study also for the 1/6 plateau [44] and found that a bound-state crystal with basis vectors $v_1 = (6, 0)$, $v_2 = (0, 4)$ [shown in Fig. 4(d)] clearly has a lower energy than the previously proposed candidates of triplet crystals [12,21,24].

Nature of the bound state and estimate of the binding energy.—The stabilization of $S_z = 2$ bound state crystals over $S_z = 1$ triplet crystals is in contradiction with the conclusions of Ref. [16], based on an expansion in J'/J, in which the authors argued that the $S_z = 2$ bound state is only energetically favorable in the dilute limit thanks to the gain in kinetic energy via a correlated hopping process, and that in a crystalline phase where the bound state is localized, the two triplets would actually repel each other. To make contact with Ref. [16], we have calculated the binding energy of a localized bound state defined by $E^{\mathrm{loc}}_{\mathrm{bind}} = E^{\mathrm{loc}}_{bs} - 2E^{\mathrm{loc}}_{\mathrm{triplet}}$, where E^{loc}_{bs} and $E^{\mathrm{loc}}_{\mathrm{triplet}}$ are the energies to form a single localized bound state and a localized triplet state for $0 \leq J'/J \leq 0.67$. These energies are estimated from simulations of a single bound state and triplet state in a 6×6 unit cell, where the repulsion between the triplets (or bound states) in neighboring cells is small, but the states remain localized within this cell [45]. As can be seen in Fig. 3, this binding energy is negative for all ratios J'/J as soon as D is large enough, so that even in the perturbative regime of Ref. [16] we predict that there is a stable localized $S_z = 2$ bound state.

To resolve the apparent contradiction, we have revisited the calculation of Ref. [16]. More precisely, we have looked at the whole excitation spectrum in the two-triplet sector, which in fact consists of four bands grouped into two pairs, separated by a large gap [44]. So, in the spirit of Wannier

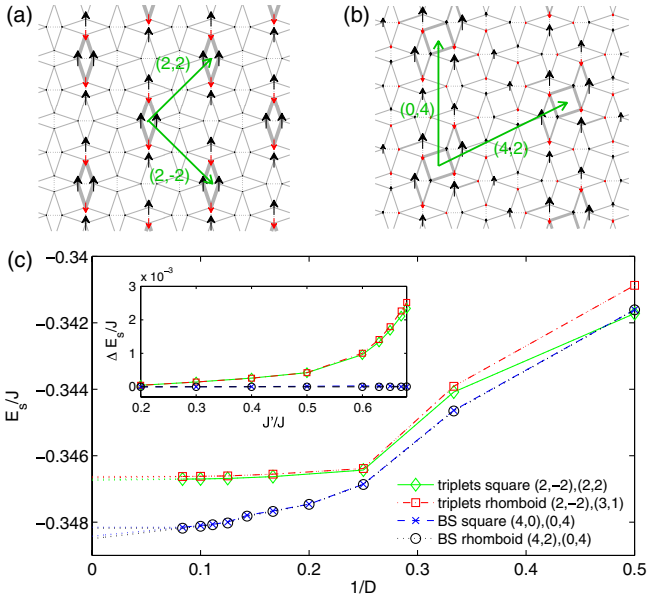

FIG. 2 (color online). Spin structures of the candidate ground states for the 1/8 plateau phase: (a) the 1/8 square crystal made of triplets with magnetic unit cell vectors $v_1 = (2, 2)$, $v_2 = (2, -2)$, (b) rhomboid crystal made of bound states (BS) defined by the vectors $v_1 = (4, 2)$ and $v_2 = (0, 4)$. (c) Variational energies per site of the competing states as a function of the inverse bond dimension $1/D$ for $J'/J = 0.63$ (the contribution from the Zeeman term has been subtracted). The unit cell vectors are given in brackets. The dotted lines are guides to the eye. The inset shows the energy difference with respect to the lowest energy state as a function of J'/J for $D = 8$.

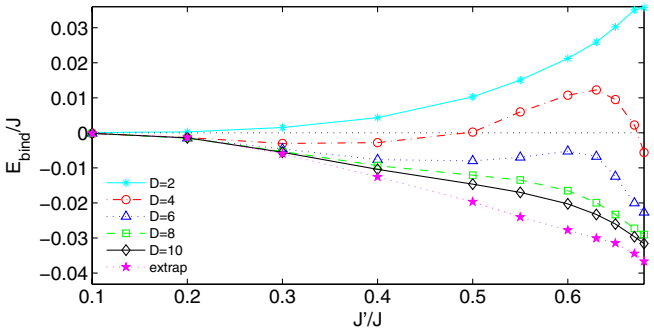

FIG. 3 (color online). Estimate of the binding energy between two $S_z = 1$ triplets as a function of J'/J, for different values of D.

functions for electronic bands, which are well localized if a band is separated from the others by a large gap, it must be possible to reconstruct well-localized wave functions from the lowest pair of bands; the energy of these localized states will be of the order of the average energy of the bands. It turns out that the average energy is always below that of two triplets [44], leading to a binding energy of the same order as our estimate for small J'/J. So, we conclude that two triplets indeed bind into a $S_z = 2$ bound state, even in a confined geometry where the bound state is not allowed to delocalize.

That the bound state we discuss is related to the bound state discussed in Ref. [16] is further confirmed by its structure [44], which goes from two second-neighbor "dressed" triplets in the small J'/J limit (as for the bound state of Ref. [16]) to the pinwheel structure of Fig. 1(b) for larger J'/J, with a central singlet plaquette reminiscent of the plaquette phase found at zero external magnetic field [46–49] for $0.675 < J'/J < 0.765$ [37]. When J'/J is large enough, there is actually an intuitive way to understand the stabilization of the bound state: in a triplet excitation, a high energy cost has to be paid on the dimer with two parallel spins [cf. Fig. 1(b)]. The bound state avoids this cost by distributing the four largest moments around a plaquette in such a way that they are neither nearest nor next-nearest neighbors, while part of the energy lost in breaking four singlets on J bonds is recovered by the formation of a singlet plaquette on J' bonds.

Magnetization curve.—Based on the previous findings it seems natural that different plateau states correspond to different crystals of bound states. For each plateau with a magnetization $2/k$, k integer, we have tested various structures (unit cell sizes) to determine the states with lowest energy. Then we have compared the variational energy of different plateaus, as a function of the external magnetic field h, to see which of the plateaus are energetically favored. The energy difference with respect to the lowest energy state as a function of h for $D = 10$ is plotted in Fig. 4(a), and the resulting magnetization curve in Fig. 4(b). Sizable magnetization plateaus appear at $1/8$, $2/15$, $1/6$, $1/5$, and $1/4$, besides the $1/3$ and $1/2$ plateaus

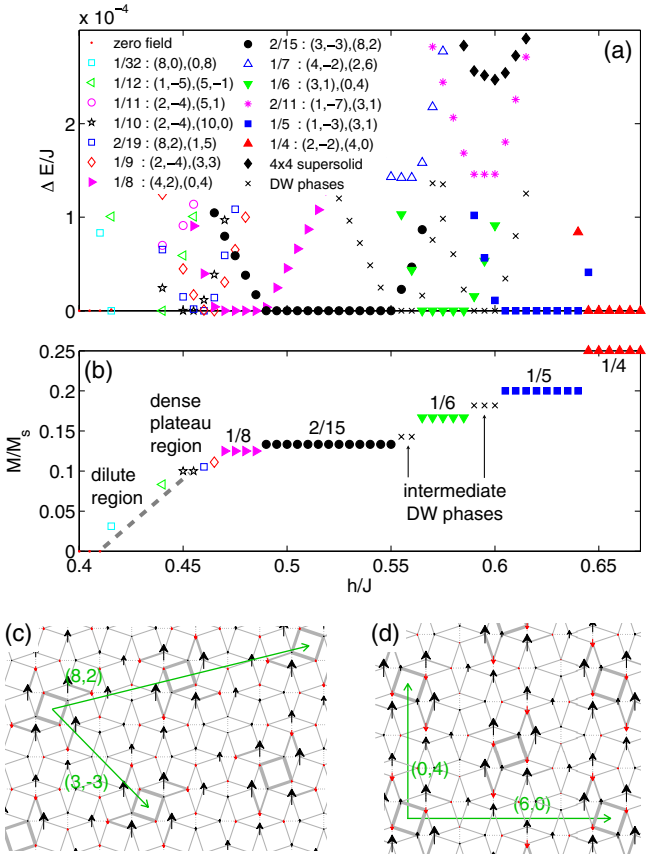

FIG. 4 (color online). (a) Comparison of the variational energies of the various competing states as a function of h with respect to the lowest energy state ($J'/J = 0.63$ and $D = 10$). The numbers in brackets in the legend show the unit vectors v_1, v_2 spanning the magnetic unit cell. (b) Magnetization curve as a function of h obtained from the lowest energy states. Sizable plateaus are found for $1/8$, $2/15$, $1/6$, $1/5$, and $1/4$, besides smaller plateaus in the lower field region. (c) Spin structure of the $2/15$ plateau state. (d) Spin structure of the $1/6$ plateau state.

at larger h [13]. The intermediate crystals $1/7$, $2/13$, $2/11$, $2/9$ are all higher in energy. The results are presented for $D = 10$. The sequence is the same for other values of D, but the sizes of the individual plateaus are very sensitive to small changes in the energy and change with D [44].

Interestingly, the spin structure of the $1/4$ plateau [44] agrees with previous results. In fact, it can be seen either as a stripe of triplets or as a stripe of bound states with unit cell vectors $v_1 = (0, 4)$, $v_2 = (1, -1)$. The same is true for the $1/3$ plateau (not shown).

Below the $1/8$ plateau we find a high density of plateaus which lie energetically very close, including plateaus at $1/12$, $1/11$, $1/10$, $2/19$, $1/9$, see Fig. 4 and [44] (the $2/17$ plateau lies slightly higher in energy). At even lower fields we enter the dilute region of bound states, where they start to delocalize (and eventually Bose condense). We did not study this region [marked by a dashed line in Fig. 4(b)] in detail.

Besides the regular crystals of bound states we find domain-wall (DW) phases (crosses in Fig. 4) between the

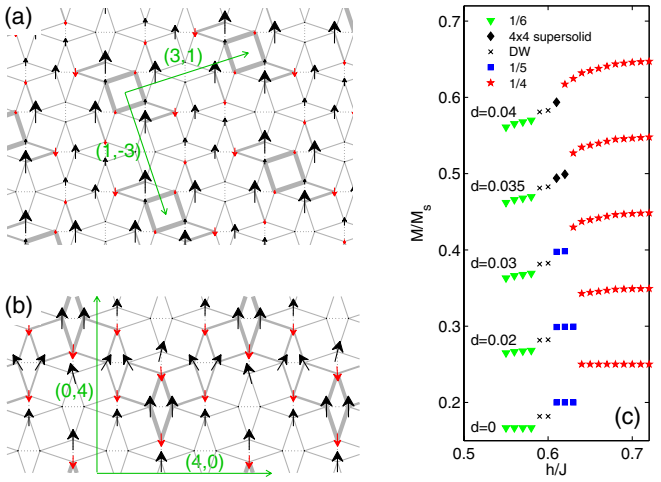

FIG. 5 (color online). (a) Spin structure of the 1/5 plateau state. (b) Spin structure of the supersolid phase in a 4×4 unit cell. (c) Effect of a intradimer Dzyaloshinskii-Moriya (DM) interaction with strength d on the magnetization curve in the vicinity of the 1/5 plateau ($D = 6$): the plateaus start to acquire a finite slope, and the 1/5 plateau disappears due to the competing 4×4 supersolid phase shown in (b) and due to the competing (deformed) 1/4 plateau state. The individual magnetization curves are shifted by 0.1 for better visibility.

2/15 and the 1/6 plateau and between the 1/6 and the 1/5 plateau. These DW phases are made of alternating domains (stripes) of the neighboring plateau states, with a magnetization depending on the individual widths of these domains. We restricted our study only to a few DW states, since these typically require very large cells. Other DW states for intermediate values of M/M_s are likely to appear between the plateaus and further reduce the size of the adjacent plateaus. Eventually, a series of domain-wall states may connect the plateaus in a smooth way, as observed experimentally [12].

We have also checked for competing supersolid phases in various cells, some of which have been found to be stable at higher magnetic fields [13]. For $J'/J = 0.63$ the only close competing supersolid phase is given by the black diamonds in Fig. 4(a), which is $> 0.0002\,J$ higher than the plateau states. Its spin structure is shown in Fig. 5(b).

Finally, we note that if we restrict our calculation to triplet crystals only, we reproduce the same sequence of magnetization plateaus as in Ref. [21] in the low-density limit of triplets ($M/M_s \leq 1/6$) (see [44]), but these states are always higher than the bound-state crystals.

Discussion.—Our predicted sequence of magnetization plateaus is in good agreement with experiments on $SrCu_2(BO_3)_2$ up to 34 T, where plateaus at 1/8, 2/15, 1/6, 1/4 have been found [12]. In particular, the 2/15 plateau appears very naturally as a regular crystal of bound states, as shown in Fig. 4(c), in contrast to the more complicated patterns of triplets proposed previously. The size of the 2/15 plateau is large compared to the experimental data. However, it is likely to get further reduced by competing domain-wall phases in larger unit cells, which we did not consider in our simulations. We cannot give a precise estimate, based on our data, of the size of the individual plateaus.

At 1/5, there is no clear sign of a sizable plateau in experiments (only a discontinuity in the slope of the magnetization curve, see Ref. [12]), whereas our simulations predict a stable plateau, with the spin structure shown in Fig. 5(a) (see [44] for a comparison with the structure found in Ref. [10]). However, in the vicinity of the 1/5 plateau there is a competing supersolid phase which is only slightly higher in energy [Fig. 5(b)]. We have studied the effect of an additional intradimer DM interaction d on this competition and got the encouraging result that even a small but realistic value between $d = 0.03\ J$ and $d = 0.04\ J$ (cf. Refs. [23,50–52]) is enough to destabilize the 1/5 plateau in favor of the supersolid phase, see Fig. 5(c). The systematic analysis including all anisotropic interactions (intra- and interdimer DM interactions and g-tensor anisotropy [52–54]) is left for future investigation.

In summary, our results are in strong support of an alternative explanation for the magnetization process in $SrCu_2(BO_3)_2$. In particular, the observed magnetization plateaus correspond to crystals of bound states and not to crystals of triplets. Structures are also proposed for the intermediate phases. The next step will be to compare the resulting structures with NMR spectra [12]. We note only that the basic requirements (spins strongly polarized along the field and spins polarized opposite to the field surrounded by weakly polarized spins) are present in all the proposed structures. Finally, our study also further demonstrates the potential of iPEPS as a powerful tool for open problems in frustrated magnetism. Thanks to (largely) unbiased simulations, unexpected physics can be discovered. The crystals of bound states found in this work definitely came as a surprise to us.

We would like to thank M. Takigawa for his critical reading of the manuscript. This work has been supported by the Swiss National Science Foundation. The simulations have been performed on the Brutus cluster at ETH Zurich.

[1] *Introduction to Frustrated Magnetism—Materials, Experiments, Theory*, Springer Series in Solid-State Sciences, edited by C. Lacroix, P. Mendels, and F. Mila (Springer-Verlag Berlin, Heidelberg, 2011), Vol. 164.
[2] B. Sriram Shastry and B. Sutherland, Physica (Amsterdam) **108B+C**, 1069 (1981).
[3] H. Kageyama, K. Yoshimura, R. Stern, N. V. Mushnikov, K. Onizuka, M. Kato, K. Kosuge, C. P. Slichter, T. Goto, and Y. Ueda, Phys. Rev. Lett. **82**, 3168 (1999).
[4] K. Onizuka, H. Kageyama, Y. Narumi, K. Kindo, Y. Ueda, and T. Goto, J. Phys. Soc. Jpn. **69**, 1016 (2000).

[5] H. Kageyama, M. Nishi, N. Aso, K. Onizuka, T. Yosihama, K. Nukui, K. Kodama, K. Kakurai, and Y. Ueda, Phys. Rev. Lett. **84**, 5876 (2000).

[6] K. Kodama, M. Takigawa, M. Horvatić, C. Berthier, H. Kageyama, Y. Ueda, S. Miyahara, F. Becca, and F. Mila, Science **298**, 395 (2002).

[7] M. Takigawa, K. Kodama, M. Horvatić, C. Berthier, H. Kageyama, Y. Ueda, S. Miyahara, F. Becca, and F. Mila, Physica (Amsterdam) **346B–347B**, 27 (2004).

[8] F. Levy, I. Sheikin, C. Berthier, M. Horvatić, M. Takigawa, H. Kageyama, T. Waki, and Y. Ueda, Europhys. Lett. **81**, 67004 (2008).

[9] S. E. Sebastian, N. Harrison, P. Sengupta, C. D. Batista, S. Francoual, E. Palm, T. Murphy, N. Marcano, H. A. Dabkowska, and B. D. Gaulin, Proc. Natl. Acad. Sci. U.S.A. **105**, 20157 (2008).

[10] L. Isaev, G. Ortiz, and J. Dukelsky, Phys. Rev. Lett. **103**, 177201 (2009).

[11] M. Jaime, R. Daou, S. A. Crooker, F. Weickert, A. Uchida, A. E. Feiguin, C. D. Batista, H. A. Dabkowska, and B. D. Gaulin, Proc. Natl. Acad. Sci. U.S.A. **109**, 12404 (2012).

[12] M. Takigawa, M. Horvatić, T. Waki, S. Krämer, C. Berthier, F. Lévy-Bertrand, I. Sheikin, H. Kageyama, Y. Ueda, and F. Mila, Phys. Rev. Lett. **110**, 067210 (2013).

[13] Y. H. Matsuda, N. Abe, S. Takeyama, H. Kageyama, P. Corboz, A. Honecker, S. R. Manmana, G. R. Foltin, K. P. Schmidt, and F. Mila, Phys. Rev. Lett. **111**, 137204 (2013).

[14] S. Miyahara and K. Ueda, Phys. Rev. Lett. **82**, 3701 (1999).

[15] T. Momoi and K. Totsuka, Phys. Rev. B **61**, 3231 (2000).

[16] T. Momoi and K. Totsuka, Phys. Rev. B **62**, 15067 (2000).

[17] Y. Fukumoto and A. Oguchi, J. Phys. Soc. Jpn. **69**, 1286 (2000).

[18] Y. Fukumoto, J. Phys. Soc. Jpn..**70**, 1397 (2001).

[19] S. Miyahara and K. Ueda, J. Phys. Condens. Matter **15**, R327 (2003).

[20] S. Miyahara, F. Becca and F. Mila, Phys. Rev. B **68**, 024401 (2003).

[21] J. Dorier, K. P. Schmidt, and F. Mila, Phys. Rev. Lett. **101**, 250402 (2008).

[22] A. Abendschein and S. Capponi, Phys. Rev. Lett. **101**, 227201 (2008).

[23] M. Takigawa, T. Waki, M. Horvatić, and C. Berthier, J. Phys. Soc. Jpn. **79**, 011005 (2010).

[24] M. Nemec, G. R. Foltin, and K. P. Schmidt, Phys. Rev. B **86**, 174425 (2012).

[25] J. Lou, T. Suzuki, K. Harada, and N. Kawashima, arXiv:1212.1999.

[26] Y. Fukumoto, J. Phys. Soc. Jpn. **69**, 2755 (2000).

[27] C. Knetter, A. Bühler, E. Müller-Hartmann, and G. S. Uhrig, Phys. Rev. Lett. **85**, 3958 (2000).

[28] K. Totsuka, S. Miyahara, and K. Ueda, Phys. Rev. Lett. **86**, 520 (2001).

[29] C. Knetter and G. S. Uhrig, Phys. Rev. Lett. **92**, 027204 (2004).

[30] S. R. Manmana, J.-D. Picon, K. P. Schmidt, and F. Mila, Europhys. Lett. **94**, 67004 (2011).

[31] F. Verstraete and J. I. Cirac, arXiv:cond-mat/0407066.

[32] J. Jordan, R. Orús, G. Vidal, F. Verstraete, and J. I. Cirac, Phys. Rev. Lett. **101**, 250602 (2008).

[33] P. Corboz, R. Orus, B. Bauer, and G. Vidal, Phys. Rev. B **81**, 165104 (2010).

[34] P. Corboz, A. M. Läuchli, K. Penc, M. Troyer, and F. Mila, Phys. Rev. Lett. **107**, 215301 (2011).

[35] P. Corboz, M. Lajkó, A. M. Läuchli, K. Penc, and F. Mila, Phys. Rev. X **2**, 041013 (2012).

[36] P. Corboz, M. Lajkó, K. Penc, F. Mila, and A. M. Läuchli, Phys. Rev. B **87**, 195113 (2013).

[37] P. Corboz and F. Mila, Phys. Rev. B **87**, 115144 (2013).

[38] G. Vidal, Phys. Rev. Lett. **91**, 147902 (2003).

[39] H. C. Jiang, Z. Y. Weng, and T. Xiang, Phys. Rev. Lett. **101**, 090603 (2008).

[40] T. Nishino and K. Okunishi, J. Phys. Soc. Jpn. **65**, 891 (1996).

[41] R. Orús and G. Vidal, Phys. Rev. B **80**, 094403 (2009).

[42] S. Singh, R. N. C. Pfeifer, and G. Vidal, Phys. Rev. B **83**, 115125 (2011).

[43] B. Bauer, P. Corboz, R. Orús, and M. Troyer, Phys. Rev. B **83**, 125106 (2011).

[44] See Supplemental Material at http://link.aps.org/supplemental/10.1103/PhysRevLett.112.147203, which includes Refs. [55,56], for the spin structures of many of the states discussed in this paper, for some additional information on the $S_z = 2$ bound state, for some technical points such as the D dependence of the magnetization curve, and for a discussion of the discrepancy between our results and those of Ref. [10].

[45] In these simulations we enforce a U(1) symmetry on the tensors, which prevents the triplets or bound states from undergoing a Bose-Einstein condensation (i.e., from completely delocalizing). We note that new techniques to study localized excitations with tensor networks have been developed [57,58], but so far they have only been tested in one dimension with matrix product states.

[46] A. Koga and N. Kawakami, Phys. Rev. Lett. **84**, 4461 (2000).

[47] Y. Takushima, A. Koga, and N. Kawakami, J. Phys. Soc. Jpn. **70**, 1369 (2001).

[48] C. H. Chung, J. B. Marston, and S. Sachdev, Phys. Rev. B **64**, 134407 (2001).

[49] A. Läuchli, S. Wessel, and M. Sigrist, Phys. Rev. B **66**, 014401 (2002).

[50] A. Zorko, D. Arčon, H. van Tol, L. C. Brunel, and H. Kageyama, Phys. Rev. B **69**, 174420 (2004).

[51] T. Rõõm, D. Hüvonen, U. Nagel, J. Hwang, T. Timusk, and H. Kageyama, Phys. Rev. B **70**, 144417 (2004).

[52] K. Kodama, S. Miyahara, M. Takigawa, M. Horvatić, C. Berthier, F. Mila, H. Kageyama, and Y. Ueda, J. Phys. Condens. Matter **17**, L61 (2005).

[53] O. Cépas, K. Kakurai, L. P. Regnault, T. Ziman, J. P. Boucher, N. Aso, M. Nishi, H. Kageyama, and Y. Ueda, Phys. Rev. Lett. **87**, 167205 (2001).

[54] J. Romhányi, K. Totsuka, and K. Penc, Phys. Rev. B **83**, 024413 (2011).

[55] W. Kohn, Phys. Rev. **115**, 809 (1959).

[56] E. I. Blount, in *Advances Solid State Physics* Vol. 13, edited by F. Seitz and D. Turnbull (Academic Press, New York, 1962), p. 305.

[57] H. N. Phien, G. Vidal, and I. P. McCulloch, Phys. Rev. B **86**, 245107 (2012).

[58] A. Milsted, J. Haegeman, T. J. Osborne, and F. Verstraete, Phys. Rev. B **88**, 155116 (2013).